FULL PAPERS

Magnetic Resonance in Medicine 41:649–656 (1999)

In Vivo ^{1}H NMR Spectroscopy of Rat Brain at 1 ms Echo Time

I. Tkáč,[1]* Z. Starčuk,[2] I.-Y. Choi,[1] and R. Gruetter[1]

Using optimized, asymmetric radiofrequency (RF) pulses for slice selection, the authors demonstrate that stimulated echo acquisition mode (STEAM) localization with ultra-short echo time (1 ms) is possible. Water suppression was designed to minimize sensitivity to B_1 inhomogeneity using a combination of 7 variable power RF pulses with optimized relaxation delays (VAPOR). Residual water signal was well below the level of most observable metabolites. Contamination by the signals arising from outside the volume of interest was minimized by outer volume saturation using a series of hyperbolic secant RF pulses, resulting in a sharp volume definition. In conjunction with FASTMAP shimming (Gruetter Magn Reson Med 1993;29: 804–811), the short echo time of 1 msec resulted in highly resolved in vivo ^{1}H nuclear magnetic resonance spectra. In rat brain the water linewidths of 11–13 Hz and metabolite singlet linewidths of 8–10 Hz were measured in 65 μl volumes. Very broad intense signals ($\Delta\nu_{1/2} > 1$ kHz), as expected from membranes, for example, were not observed, suggesting that their proton T_2 are well below 1 msec. The entire chemical shift range of ^{1}H spectrum was observable, including resolved resonances from alanine, aspartate, choline group, creatine, GABA, glucose, glutamate, glutamine, myo-inositol, lactate, N-acetylaspartate, N-acetylaspartylglutamate, phosphocreatine, and taurine. At 9.4 T, peaks close to the water were observed, including the H-1 of α-D-glucose at 5.23 ppm and a tentative H-1 resonance of glycogen at 5.35 ppm. Magn Reson Med 41:649–656, 1999.

Key words: ^{1}H NMR spectroscopy; short echo time STEAM; water suppression; highly resolved spectra; rat brain

In vivo ^{1}H NMR spectroscopy has developed into a useful tool for measuring changes in several metabolites (1,2). Localization methods with TEs of 135–270 ms have been applied, yielding information on metabolites such as N-acetylaspartate (NAA), creatine (Cr), choline (Cho), and lactate (Lac) (3,4). With decreasing TE, spectral information increases considerably, and the measurement of metabolites with coupled spin systems such as glutamate (Glu), glutamine (Gln), myo-inositol (Ins), and glucose (Glc) becomes feasible (5,6). Generally, a TE ranging from 20 to 40 ms is considered short for most in vivo applications. Several studies with TEs of 5–10 ms have been reported (7–10). Short echo time localization methods minimize T_2 relaxation effects, which increases the sensitivity and reliability of metabolite quantitation. Short echo time is essential for the detection of metabolites with larger molecular weight, e.g., glycogen, whose T_2 is on the order of milliseconds in the model systems (11). Minimized TE may also be important for the detection of molecules with strongly coupled spin systems, e.g., glutamate.

The minimum echo time is determined by the radiofrequency (RF) pulse duration needed for volume of interest (VOI) selection and by the minimum duration of spoiler gradients sufficient to dephase the unwanted magnetization from outside the VOI. This usually translates into requirements on gradient system performance, e.g., the strength and rise time of the field gradients and the elimination of eddy currents.

For the potential ^{1}H NMR detection of glycogen we sought to develop a highly robust localization method with substantially reduced echo time compared with previous studies and also to demonstrate detection of the glucose/glycogen resonance close to the water signal. For this purpose we developed a highly efficient water suppression with reduced sensitivity to B_1 variation and thus suitable for surface coil [variable pulse power and optimized relaxation delays (VAPOR)]. Minimization of the water signal and any artifacts arising outside of the VOI permitted reliable detection of resonance signals in the whole range of ^{1}H chemical shifts, particularly very close to water signal.

MATERIALS AND METHODS

All measurements were performed at 400 MHz on a Varian (INOVA) imaging spectrometer equipped with 9.4 T magnet (Magnex Scientific) with 31 cm bore. An actively shielded, 11 cm inner diameter gradient coil (Magnex Scientific) with a rise time of 500 μs to the maximum field gradient strength of 300 mT/m was used, giving triangular shaped gradient pulses with a peak strength of 100 mT/m with less than 300 μs overall duration. The time of the first data point was carefully optimized so that only zero-order phase correction was necessary. The free induction decays (FIDs) were not corrected for eddy currents, and the drift of the field caused by the eddy currents was less than 1 Hz (12). A quadrature surface RF coil (transmitting/receiving) with two loops of 14 mm diameter was used for the excitation and detection, built according to a recently described design (13). Adjustment of first- and second-order shim coil currents was performed using a fully adiabatic version of FASTMAP (14). The field homogene-

[1]Center for Magnetic Resonance Research, Department of Radiology, University of Minnesota, Minneapolis, Minnesota.

[2]Institute of Scientific Instruments, Academy of Sciences of the Czech Republic, Brno, Czech Republic.

Grant sponsor: W.M. Keck Foundation; Grant sponsor: NIH; Grant number: P41 RR08079.

*Correspondence to: Ivan Tkáč, Center for Magnetic Resonance, Dept. of Radiology, University of Minnesota, 2021 6th Street SE, Minneapolis, MN 55455. E-mail: ivan@cmrr.umn.edu

Received 16 June 1998; revised 28 September 1998; accepted 4 November 1998.

ity in a 22–130 μl VOI typically resulted in signal line widths of 11–13 Hz for water and 8–10 Hz for metabolite singlets in vivo.

To adjust and test the pulse sequence, a cylindrical two-chamber phantom filled with 10 mM creatine (inner volume) and 30% ethanol (outer volume) was used. Male Sprague-Dawley rats (200–300 g) were anesthetized by a gas mixture of O_2/N_2O 2:1 with 1% isoflurane. The rats were intubated and actively ventilated. The physiological status of the animal was monitored using a pulse oximeter (Nonin Medical) attached to a tail. The temperature of the animal was maintained at 37°C by warm water circulation and verified by rectal temperature sensor (Cole-Palmer). Glucose was infused into the femoral vein at a rate of 10 mg/min.

RESULTS

Pulse Sequence

The inhomogeneity of the B_1 field generated by the quadrature surface coil was taken into account for the design of water suppression and localization sequence. The pulse sequence consists of seven chemical shift-selective (CHESS) RF pulses followed by crusher gradients interleaved with three outer volume saturation (OVS) modules and localizing stimulated echo acquisition mode (STEAM) sequence, as shown by the scheme

$$4 \times \text{CHESS—OVS—CHESS—OVS} —$$

$$-2 \times \text{CHESS—OVS—STEAM—ACQ}$$

Minimization of Echo Time

The STEAM sequence was designed for an extremely short echo time. To reduce the effective echo time to 1 msec, we implemented asymmetric numerically optimized RF pulses (15), shown in Fig. 1a. The shape of the asymmetric 90° RF pulse was derived from a symmetric 90° pulse in a way proposed for the construction of asymmetric 180° RF pulses (16). The shape of the symmetric 90° pulse was constructed by superposition of a low number of Gaussian-weighted cosines (17). The template of the asymmetric pulse is available and will be published in a forthcoming paper. These pulses have a significantly improved excitation profile compared with a standard five-lobe sinc pulse (Fig. 1b). A 500 μs 90° pulse required 3.3 kHz peak power ($\gamma B_1/2\pi$) and provided a bandwidth of 13.5 kHz. The STEAM pulse sequence used for echo time 1 ms is shown in Fig. 2.

The strength of the slice-selection gradients for VOI localization was close to 100 mT/m, which reduced displacement of the VOI to less than ±0.2 mm in all three directions for a 5 ppm chemical shift range at 400 MHz, which can be considered negligible relative to the size of the VOI.

An optional Gaussian CHESS pulse was added to the TM period for further suppression of water magnetization. It is especially useful for the experiments with longer TM period when the recovery of water M_z magnetization due to T_1 relaxation during TM is not possible to neglect. Increased water M_z magnetization is detected as an FID from the last slice excitation, which might be not removed perfectly by phase cycling and/or crusher gradients due to the very short echo time.

Water Suppression

Previous water suppression methods typically used three to four (CHESS) pulses and were designed for modest RF inhomogeneity (10% B_1 variation) of a volume coil (18). The new water suppression scheme is based on the combination of selective pulses with different RF power similarly to recent reports (18–21). However, the number of pulses, the difference in RF power, and the timing were significantly modified. The main goal of the new water suppression design was to decrease the sensitivity to applied RF power, to suppress the water signal efficiently by inhomogeneous B_1 field of the surface transmitting coil.

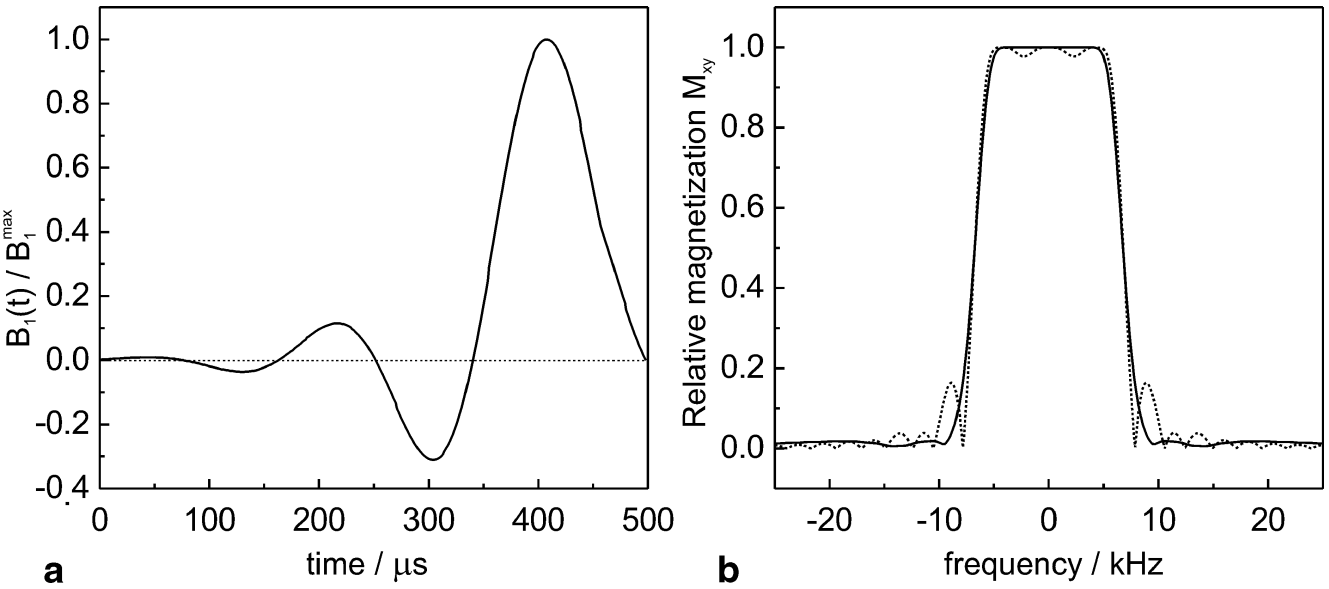

FIG. 1. (**a**) The pattern of the asymmetric 500 μs RF pulse, the relative amplitude of the real part of B_1 vs. time. (**b**) The excitation profile of the asymmetric 500 μs RF pulse (solid line) compared to the profile of the 5 lobe sinc RF pulse of the same bandwidth (dotted line).

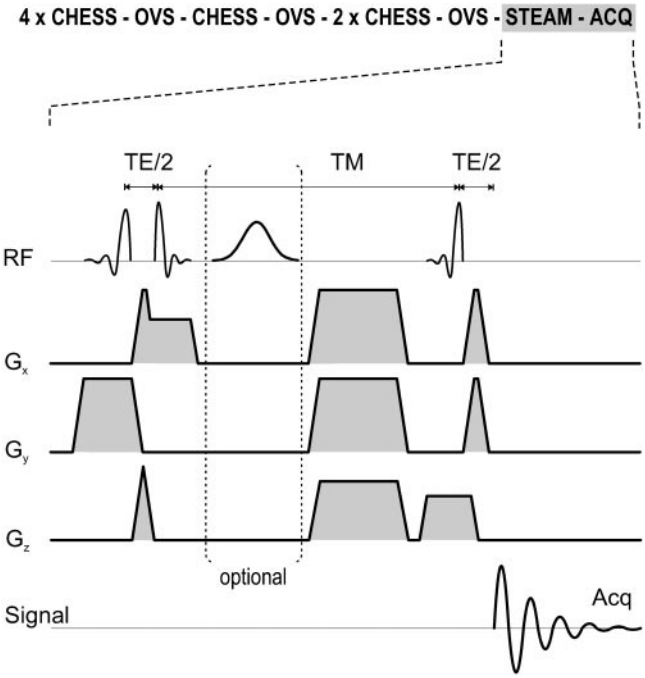

FIG. 2. The scheme of STEAM localizing sequence with asymmetric RF pulses designed for echo time 1.0 ms. The Gaussian CHESS pulse in TM period is optional.

The resulting optimized water suppression scheme has seven CHESS pulses (Fig. 3). The applied RF power of the seven pulses varied by 5 dB, i.e., 1.78-fold in peak B_1. The delays t1–t7 between the consecutive pulses are shown in Fig. 3.

The relaxation of water (T_1 = 1–2 s) was taken into account for the optimization and simulation. The calculated trajectories of M_z magnetization at different B_1 field strengths (different nominal flip angles) are plotted in Fig. 3.

The three M_z components exposed to different B_1 fields cross the zero value almost at the same time. The coarse adjustment of water suppression was done by simultaneously increasing the power of all seven CHESS pulses. Water M_z magnetization after the seventh CHESS pulse is slightly negative but approaches zero due to the T_1 relaxation. The fine adjustment of water suppression was performed by optimizing the last time delay t7.

The calculated intensity of the residual water signal as a function of nominal flip angle is plotted in Fig. 4. Comparison with the water suppression enhanced through T_1 effects (WET) method with four CHESS pulses of variable flip angles (18) and with the standard water suppression scheme with three identical CHESS pulses clearly shows the efficiency and the ability of the new sequence to suppress the unwanted water signal for a broad range of flip angles. This new water suppression scheme is also insensitive to T_1 variation. For instance, the relative residual water magnetization is less than 2% for T_1 ranging from 1 to 2 s and for a nominal flip angle from 65 to 125°.

Asymmetric RF pulses, identical to those used for slice selection in STEAM, were used for the water suppression. The advantage of an excellent excitation profile was the decreased sensitivity to the misadjustment of frequency of CHESS pulses. The water suppression scheme affected M_z magnetization by less than 5% outside a 400 Hz bandwidth (1 ppm) when using 20 ms RF pulses, as shown in Fig. 5. The crusher gradients after CHESS pulses were carefully selected in a different axis (x, y, or z) and different strength to avoid the generation of unwanted stimulated and spin echoes of the water signal (22).

Outer Volume Saturation

To improve the localizing performance and reduce the demands for crusher gradients in the localization sequence, OVS pulse train modules were added to the pulse

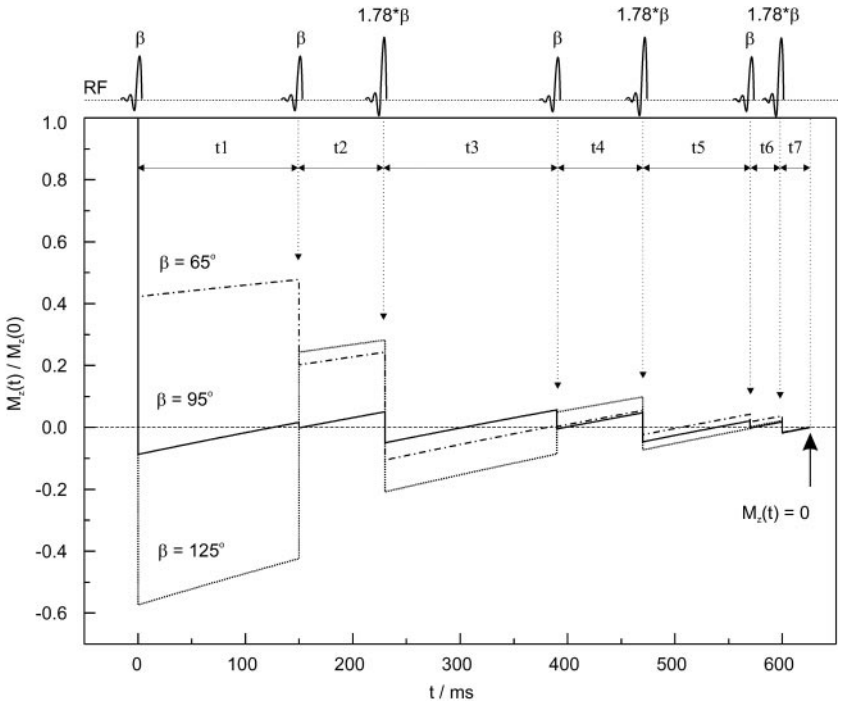

FIG. 3. Seven CHESS water suppression scheme (VAPOR) with optimized flip angles and timing. Calculated time dependence of the water M_z magnetization for three different values of nominal flip angle (different B_1 of the RF coil). Optimized time delays t1 = 150 ms, t2 = 80 ms, t3 = 160 ms, t4 = 80 ms, t5 = 100 ms, t6 = 30 ms, t7 = 26 ms.

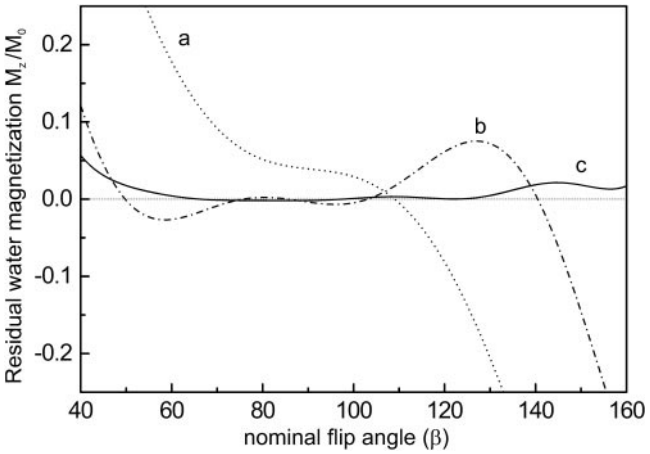

FIG. 4. Calculated dependence of the residual water M_z magnetization on nominal flip angle. Line a, Standard CHESS pulse scheme with three identical RF pulses and equal delays of 60 ms; Line b, WET method with 4 CHESS pulses of different flip angle $\beta - 1.25*\beta - 0.85*\beta - 1.98*\beta$ and equal delays of 60 ms; Line c, seven CHESS pulse scheme (VAPOR) with variable flip angle and optimized timing according the Fig. 3. A relaxation time $T_1 = 1.5$ s was used for the calculation.

sequence. Three OVS modules were interleaved with CHESS elements. Each OVS module consisted of six hyperbolic secant (hs) pulses to saturate the six slices adjacent to the volume of interest. The hs pulses were selected for their broad bandwidth and sharp profile. Broad bandwidth hs pulses (18.5 kHz for 1.2 ms pulse width) permitted the use of strong field gradients for the selection and minimization of the chemical shift displacement error, which was thus <0.5 mm for 5 ppm. Use of hs pulses further reduced the peak B_1 requirements for 90° pulses by twofold compared with sinc pulses of the same bandwidth (~20 kHz). In addition, the transverse magnetization generated by the hs pulse has a quadratic phase frequency relationship, which is advantageous for dephasing. In the second OVS module the RF power was increased by 6 dB to decrease B_1 sensitivity of OVS. The full-passage hs pulses were used for ~90° excitation in a non-adiabatic manner. The power of the RF pulses was adjusted by replacing the final localizing sequence with an imaging spin echo sequence. Hence the profile of the object in three orthogonal directions x, y, and z was measured and the RF power for OVS adjusted. As an example, Fig. 6 shows the dependence of the x profile on the applied power of the OVS pulses. For similar coil loading the optimal power is similar and it was not necessary to control the setting, once it was adjusted.

The increased number of CHESS elements and OVS modules improved the localization performance and efficiency of water suppression, but at the same time increased the possibility of unwanted stimulated echo generation (22). For this reason crusher field gradients were set and adjusted very carefully, such that the whole preparation part of the sequence before the STEAM localization became highly asymmetric. Such unwanted signals were traced during pulse sequence development by adding a read gradient at the end of the sequence and measuring VOI profiles. The time domain data revealed the location of the unwanted rephasing in k-space. These echoes can be moved from the area close to the center of k-space by changing a suitable crusher gradient. Then the probability of unwanted rephasing due to B_0 inhomogeneity is highly reduced.

Phantom Study

A two-chamber phantom was used to test sequence performance and to eliminate residual unwanted signals by adjustment of crusher amplitudes. The VOI (65 μl) was positioned in the inner volume 1 mm adjacent to the interface with the outer volume (Fig. 7). The ^{1}H NMR spectrum of the phantom measured without the localization is shown in Fig. 8.

Localization performance of the pulse sequence and the importance of the outer volume saturation are demonstrated by the spectra (Fig. 8b,c). Without OVS, the spectrum (Fig. 8b) is contaminated by the ethanol resonances arising outside of the VOI. The lower trace (Fig. 8c) measured with the complete pulse sequence is void of an ethanol signal, in spite of 100 times higher concentration of ethanol compared with creatine.

In Vivo Experiments

A typical in vivo ^{1}H NMR spectrum of the rat brain measured with echo time 1 msec is shown in Fig. 9. The 65

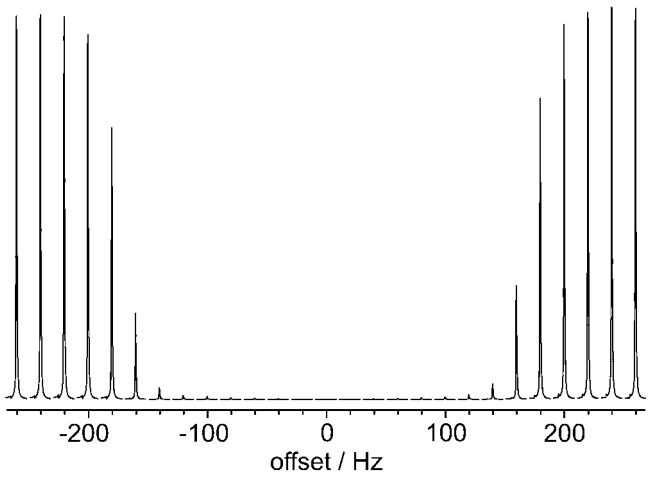

FIG. 5. Frequency selectivity of the seven CHESS water suppression with asymmetric RF pulses shown in Fig. 1a. (pw = 20 ms, frequency increment in arrayed experiment was 20 Hz.)

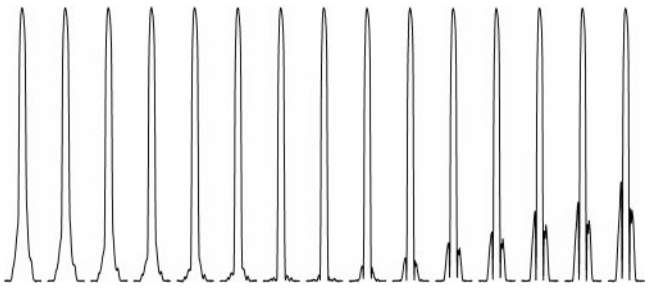

FIG. 6. Adjustment of the RF power of OVS pulses. The dependence of profile in x direction on the RF power of OVS pulses. The power is increased from left to right by 1 dB.

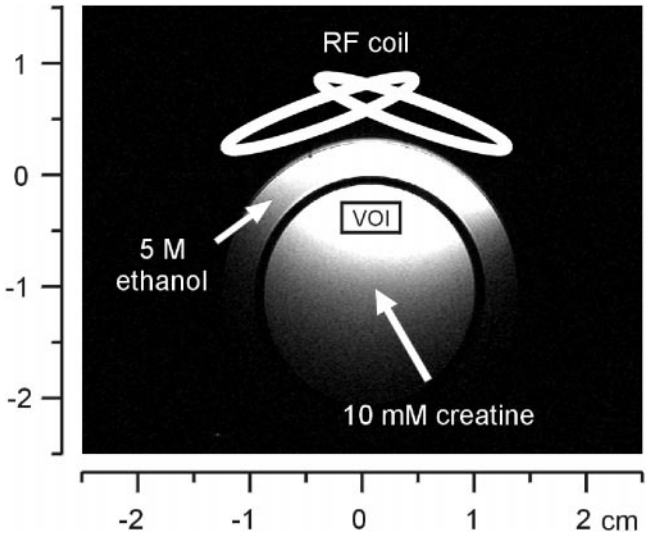

FIG. 7. The MR image of the two chamber phantom (FLASH, TE = 7 ms, TR = 50 ms). The position of the VOI and of the quadrature surface RF coil is depicted as used for the test measurements.

μl (5.0 × 2.6 × 5.0 mm^2) voxel was located on the midline of the brain, 2 mm posterior to bregma and 3 mm ventral to it. As in this spectrum, the intensity of the residual water signal was always much lower than the signal intensity of the main metabolites. The measurement of the entire chemical shift range in ^1H spectra was possible due to the elimination of unwanted signals generated outside the VOI. All signals outside the region ±0.5 ppm from the water signal (δ = 4.65 ppm) were not affected by the VAPOR water suppression, allowing for the direct observation of brain glucose at 5.23 ppm (23) as well as the feasibility of measuring other resonances in this region, such as glycogen (24,25).

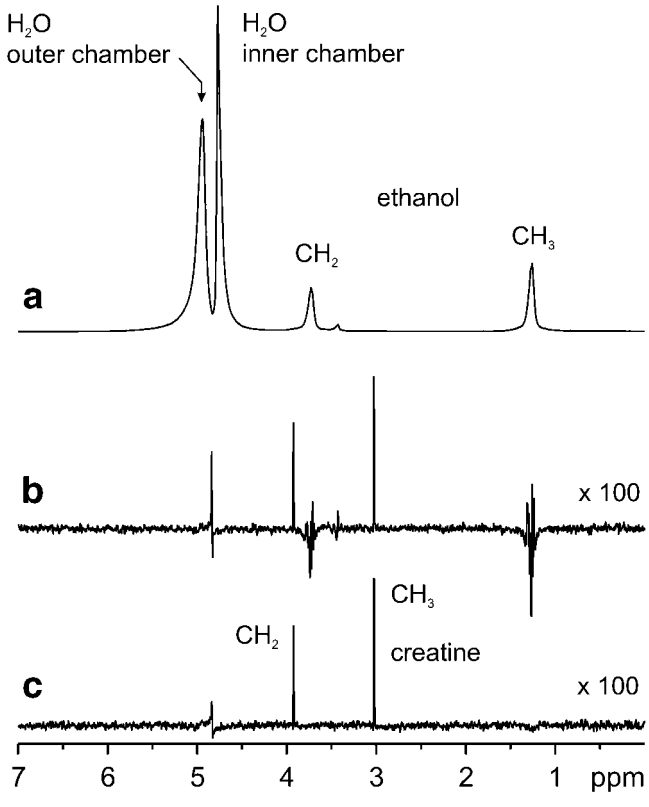

FIG. 8. ^1H NMR spectra of the two chamber phantom. (**a**) Spectrum measured without localization (pulse and acquire sequence). (**b**) Spectrum measured with VAPOR − STEAM sequence without the OVS (VOI = 65 μl, number of scans = 4, vertical scale is increased 100 × relative to upper trace). (**c**) Spectrum measured with the full pulse sequence, including the OVS, parameters are the same as (b).

Water suppression was further improved by placing an additional CHESS pulse during the TM period. In addition, a prolonged TM period decreased the contribution of very broad signals, probably due to fast T_1 relaxation, and thus made the baseline of the spectrum flatter (not shown).

The expanded region of the spectrum from 0.7 to 4.3 ppm (Fig. 9a) demonstrates that the high spectral resolution was preserved at a TE of 1 ms. Despite the short echo time, the multiplet fine structure of the resonances of myo-inositol (3.52 ppm, 3.62 ppm, 4.05 ppm), taurine (Tau, 3.42 ppm), NAA (2.49 ppm, 2.67 ppm), glutamine (2.44 ppm), and glutamate (2.34 ppm) is observable. However, it is also possible to distinguish creatine (3.92 ppm) from phosphocreatine (PCr, 3.93 ppm), N-acetylaspartylglutamate (NAAG, 2.05 ppm) from NAA (2.01 ppm), and the overlapped signals near 3.25 ppm, which are choline groups (3.19 ppm), taurine (3.25 ppm), and myo-inositol (3.27 ppm). Lactate signal at 1.32 ppm was always resolvable from the macromolecule background (Fig. 9), indicating that steady-state lactate concentration is NMR detectable in the brain of healthy intact rats under physiological conditions at 9.4 T. A detailed assignment and quantitative analysis is beyond the scope of this paper.

The ^1H spectrum measured at 1 ms echo time contains an increased contribution from fast relaxing macromolecule resonances. The pattern closely corresponds to the spectrum of cerebral cytosol after dialysis in which the signals were assigned mainly to proteins (26). Spectra measured at different echo times from 1 to 20 ms are shown in Fig. 10.

The contribution of macromolecule resonances decreased rapidly with increasing echo time. In addition, significant signal changes resulted from J-modulation of strongly coupled spin systems, such as the 3 and 3' protons of glutamate near 2.05 ppm, or the 3 and 3' protons of N-acetyl aspartate at 2.49 and 2.67 ppm. Phantom spectra observed from a solution of glutamate showed that the signal intensities of the 3 and 3' protons in spectra with line-broadening typical for in vivo spectra were attenuated by 15% and 57% when the echo time was prolonged from 1 to 10 and 20 ms, respectively (Fig. 11).

The signals H-1 of α-D-glucose and NH of NAA were the most significant in the region from 5 to 9 ppm. The spectrum in Fig. 9 was measured during glucose infusion. In normal rat brain the glucose concentration is roughly three times lower than in plasma (27) and varies with the level of plasma glucose as in human brain (28). The downfield broad shoulder of glucose resonance at 5.35 ppm was regularly observed in short echo time experiments (Fig. 9b). The chemical shift of this broad resonance is consistent with the chemical shift of the H-1 signal of glycogen.

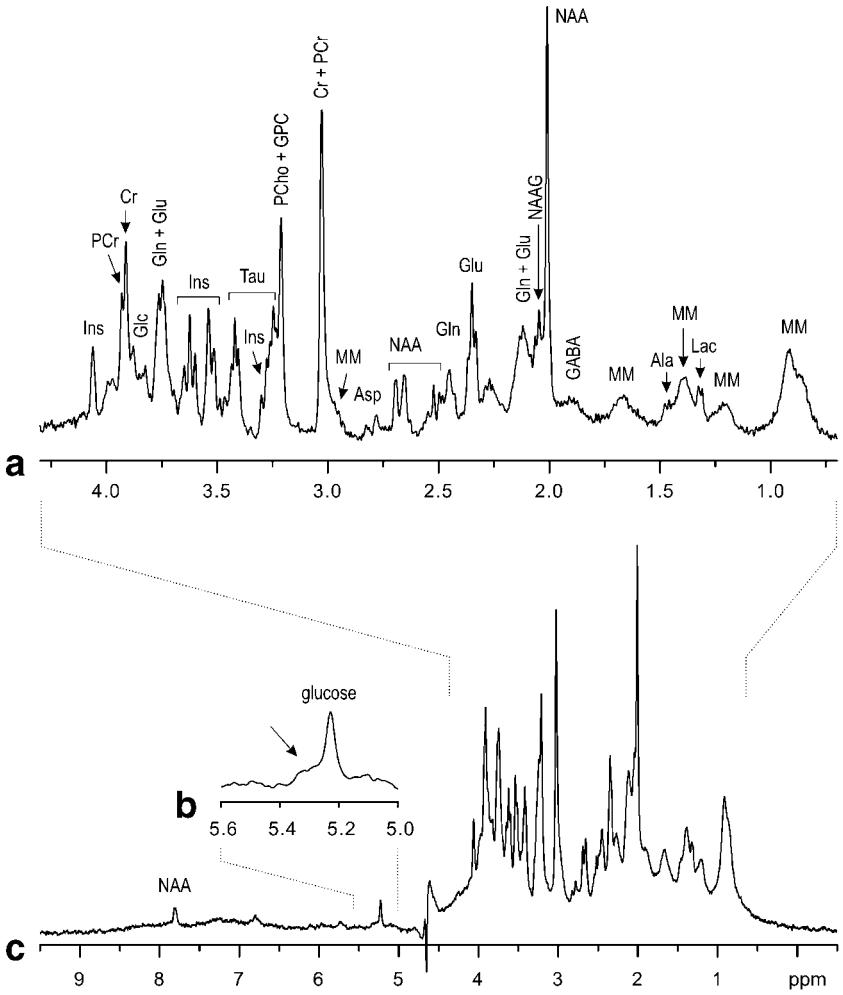

FIG. 9. In vivo ^{1}H NMR spectrum of the rat brain measured by the STEAM sequence with the echo time 1.0 ms. TM = 5 ms, TR = 4 s, NT = 320, VOI = 65 μl. Only zero order phase correction was applied after FT. (**a**) Shifted Gaussian function (gf = 0.2, gsf = 0.1) used for resolution enhancement. (**b**) Expanded spectral region with glucose resonance, the arrow is pointing to a broad resonance consistently observed, exponential multiplication lb = 8 Hz, (**c**) the whole spectrum, lb = 3 Hz.

DISCUSSION

The combination of high magnetic field, strong field gradients with reduced residual eddy current effects, sensitive RF coil, higher order shimming (FASTMAP), and the developed pulse sequence enabled us to measure routinely highly resolved ^{1}H NMR spectra at echo times as short as 1 msec (Fig. 9). Asymmetric RF pulses were the basis to achieve the ultra-short echo time, because only 15% of the total pulse duration time is effective in the echo time period and therefore rephasing gradient requirements were greatly reduced (Fig. 2). The improved square-like excitation profile of the asymmetric RF pulses (Fig. 1b) maximized the signal and improved the localization performance due to reduced intensities of the side lobes. However, outer volume saturation is still necessary to eliminate completely signal outside the VOI (Fig. 8). At the same time, the OVS reduces the demands on crusher gradients needed to suppress the FID after the last slice-selective pulse of STEAM.

The measurement of the whole chemical shift range in ^{1}H spectra is feasible due to the excellent water suppression and elimination of any signals arising outside the VOI, which allowed the reliable detection of glucose in rat brain by the direct observation of the H-1 resonance of the α-anomer at 5.23 ppm as in human brain (23). More than 80% of the signal intensity of glucose is grouped in the chemical shift region 3.2–3.9 ppm (29). However, the signals are broad due to spin-spin coupling and inherent linewidth. In addition, the signals are overlapped by much stronger resonances of glutamate, glutamine, myo-inositol, and taurine, which may render direct quantitation of glucose rather complex in the upfield spectral region.

Signal intensity of the broad resonance at 5.35 ppm (Fig.9b) was similar to that of glucose when no infusion was applied. This is consistent with a brain glycogen concentration of approximately 4–5 μmol/g glucosyl units (30,31), when taking into account reduced NMR visibility of glycogen (~30% observed at 37°C in phantom). A study reported glycogen H-1 signal in in vivo ^{1}H NMR spectra of rat liver (32). However, this broad signal is also consistent with the chemical shift of th CH = CH group of olefinic free fatty acids (33). Nevertheless, a broad signal between 3.3 and 4.1 ppm was observed in the spectrum of a patient with phosphorylase deficiency (34), which is consistent with the spectrum of the protons H-2 to H-6 of glycogen. Further experiments are necessary to ascertain the ^{1}H NMR visibility of brain glycogen in vivo.

Short echo time in vivo ^{1}H NMR spectra of the rat brain at 9.4 T have increased macromolecule signals ($\Delta\nu_{1/2} \sim 50$ Hz), ascribed to proteins (26), but very broad signals ($\Delta\nu_{1/2} > 1$ kHz) deteriorating the spectral baseline were not observed (Fig. 9). Therefore, the relaxation of membrane

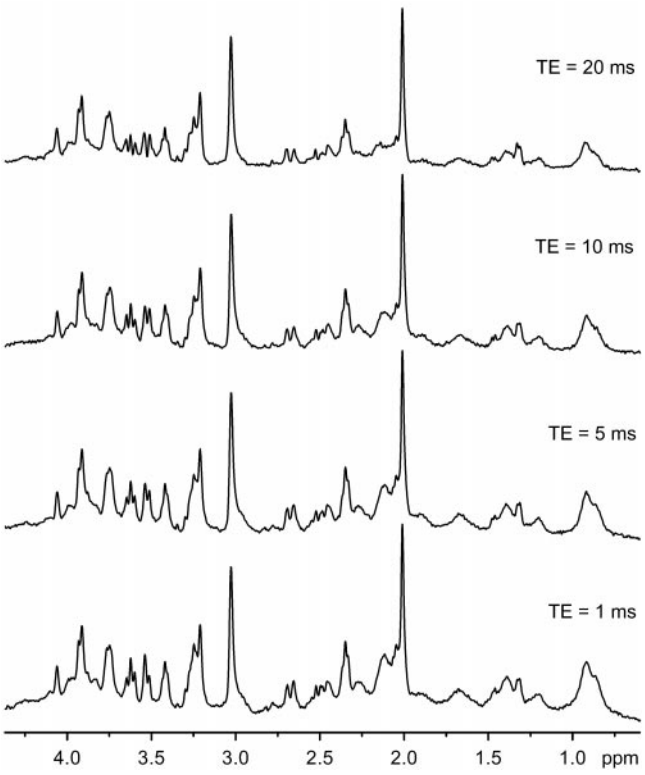

FIG. 10. Dependence of in vivo ^{1}H NMR spectra of the rat brain on the echo time. VAPOR − STEAM, VOI = 65 µl, TM = 5 ms, TR = 4 s, NT = 320, gf = 0.2.

compounds, for example, should be $T_2 < 1$ ms. The short echo time localization sequence is advantageous for quantitative analysis because T_2 relaxation effects are minimized. In addition, the water signal measured by the STEAM sequence (without water suppression) at echo time 1 msec is less likely to be affected by T_2 changes and thus may be a more robust internal reference for metabolite quantitation.

Ultra short echo time is very important for the detection of coupled spin systems such as glutamate (Fig. 10, 11), glutamine, γ-aminobutyric acid, myo-inositol, taurine, and glutathione, because the signal intensity decreases and phase distortions caused by J-modulation are minimized (35,36). In addition, the metabolite spectra required as prior knowledge to several fitting procedures are easier simulated, once the database of chemical shifts and coupling constants is accurately determined (37).

The seven-pulse water suppression scheme (VAPOR), depicted in Fig. 3, is highly efficient, robust, and easy to adjust. Using variable RF power (5 dB difference) and optimized timing with respect to T_1 relaxation results in efficient water suppression insensitive to threefold B_1 variations. The decreased sensitivity of the water suppression to B_1 inhomogeneity enabled use of a surface coil as transceiver, allowing higher peak B_1. Similar improvements of CHESS, such as WET (18) and other methods were designed and optimized for ~10% B_1 variation, which may be adequate for volume RF coils but definitely is not suitable for surface coil transceiver. The proposed water suppression scheme has a higher sensitivity to B_1 than the

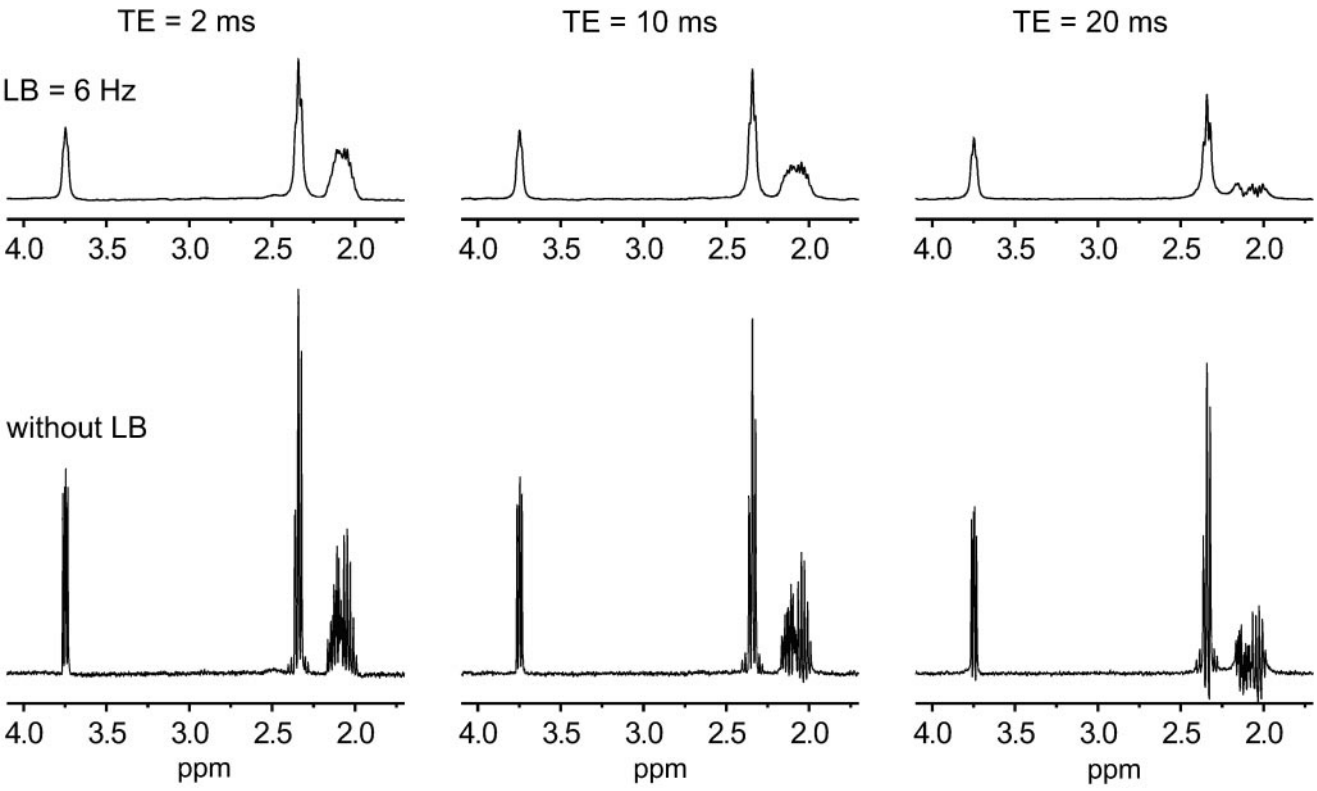

FIG. 11. ^{1}H NMR spectra of the glutamate phantom (50 mM, pH = 7.10, T = 37.0°C) measured at increasing echo time from 2 to 20 ms; STEAM, TM = 5 ms, VOI = 65 µl, NT = 64. The changes of the line shape are caused by J-modulation. Lower traces—only FT applied. Upper trace—line broadening of 6 Hz (exponential multiplication) resulting in line widths identical to those in vivo ^{1}H spectra.

BISTRO technique with adiabatic pulses (38), but its advantage is that it takes into account the T_1 relaxation of water. Recent reports showed that prolonged RF saturation leads to magnetization transfer effect on several metabolites (39). However, the changes in signal intensities when using one TM CHESS pulse instead of all seven pulses before the STEAM sequence were within 5%. For clinical applications at lower magnetic field, the proposed VAPOR scheme can be used to achieve high-quality water suppression without the need for careful RF power adjustment, which can significantly increase the quality and reliability of clinical MR spectroscopy. The general clinical applicability of the proposed scheme was verified by a preliminary implementation of this pulse sequence on a whole-body 4T MR system. Despite the 7 CHESS and 18 OVS RF pulses, the modestly increased specific absorption rate was still well below the Food and Drug Administration guidelines. It is obvious that the water suppression scheme interleaved with OVS is not specific for STEAM and can be used in combination with other localizing methods.

CONCLUSIONS

We conclude that high-resolution high-quality ^{1}H NMR spectra can be acquired from rat brain at TE = 1 msec, thereby improving quantification reliability. Seven selective RF pulses of variable power and optimized timing (VAPOR) efficiently suppress the water signal in spite of B_1 inhomogeneity of the surface coil and permit the detection of signals in nearly the entire proton chemical shift range, including signals close to the water resonance. Provided that ^{1}H NMR visibility is sufficiently high, the proposed sequence should permit detection of brain glycogen signals, for example. The improvements to ^{1}H NMR localization presented are applicable to other localization methods such as PRESS and to clinical situations.

REFERENCES

1. Howe FA, Maxwell RJ, Saunders DE, Brown MM, Griffiths JR. Proton spectroscopy in vivo. Magn Reson Q 1993;9:31–59.
2. Van Zijl PC, Barker PB. Magnetic resonance spectroscopy and spectroscopic imaging for the study of brain metabolism. Ann NY Acad Sci 1997;820:75–96.
3. Hennig J, Pfister H, Ernst T, Ott D. Direct absolute quantification of metabolites in the human brain with in vivo localized proton spectroscopy. NMR Biomed 1992;5:193–199.
4. Ross B, Michaelis T. Clinical applications of magnetic resonance spectroscopy. Magn Reson Q 1994;10:191–247.
5. Michaelis T, Merboldt KD, Bruhn H, Hanicke W, Frahm J. Absolute concentrations of metabolites in the adult human brain in vivo: quantification of localized proton MR spectra. Radiology 1993;187:219–227.
6. Gyngell ML, Ellermann J, Michaelis T, Hanicke W, Merboldt KD, Bruhn H, Frahm J. Non-invasive ^{1}H NMR spectroscopy of the rat brain in vivo using a short echo time STEAM localization sequence, NMR Biomed 1991;4:150–156.
7. Seeger U, Klose U, Seitz D, Nägele T, Lutz O, Grodd W. Proton spectroscopy of human brain with very short echo time using high gradient amplitudes. Magn Reson Imaging. 1998;16:55–62.
8. Starčuk Z, Tkáč I, Starčuk Z Jr. Whole chemical shift range in vivo ^{1}H MR spectroscopy of the rat brain. MAGMA 1997;Suppl 5:166.
9. Dixon RM, Frahm J. Localized proton MR spectroscopy of the human kidney in vivo by means of short echo time STEAM sequence. Magn Reson Med 1994;31:482–487.
10. Gideon P, Danielsen ER, Schneider M, Henriksen O. Short echo time proton spectroscopy of the brain in healthy volunteers using an insert gradient head coil. Magn Reson Imaging 1995;13:105–109.
11. Chen W, Zhu X-H, Avison MJ, Shulman RG. Nuclear magnetic relaxation of glycogen H1 in solution. Biochemistry 1993;32:9417–9422.
12. Terpstra M, Andersen PM, Gruetter R. Localized eddy current compensation using quantitative field mapping. J Magn Reson 1998;131:139–143.
13. Adriany G, Gruetter R. A half volume coil for efficient proton decoupling in humans at 4 Tesla. J Magn Reson 1997;125:178–184.
14. Gruetter R. Automatic, localized in vivo adjustment of all first- and second-order shim coils. Magn Reson Med 1993;29:804–811.
15. Starčuk Z Jr, Starčuk Z. Optimized asymmetric slice selective 90° and 180° RF pulses for localized MR spectroscopy. In: Proceedings of the SMR 2nd Annual Meeting, San Francisco, 1994. p 1137.
16. Starčuk Z Jr, Bartušek K, Starčuk Z. Asymmetric amplitude-modulated radiofrequency pulses and their application to band-selective decoupling. J Magn Reson A 1993;104:340–344.
17. Starčuk Z, Puček L, Starčuk Z Jr. New symmetric frequency-selective RF pulses for population inversion. J Magn Reson 1988;80:352–358.
18. Ogg RJ, Kingsley PB, Taylor JS. WET, a T_1- and B_1-insensitive water-suppression method for in vivo localized ^{1}H NMR spectroscopy. J Magn Reson B 1994;104:1–10.
19. Ernst T, Hennig J. Improved water suppression for localized in vivo ^{1}H spectroscopy. J Magn Reson B 1995;106:181–186.
20. Shen JF, Saunders JK. Double inversion recovery improves water suppression in vivo. Magn Reson Med 1993;29:540–542.
21. Starčuk Z Jr, Tkáč I, Starčuk Z. Localized proton MR spectroscopy: Short echo-time STEAM sequence with a new approach to T_1 insensitive highly effective water suppression. In: Proceedings of the ISMRM 5th Annual Meeting, Vancouver, 1997. p 1459.
22. Kingsley PB. Magnetic field gradients and coherence-pathway elimination. J Magn Reson B 1995;109:243–250.
23. Gruetter R, Garwood M, Ugurbil K, Seaquist ER. Observation of resolved glucose signals in ^{1}H NMR spectra of the human brain at 4 Tesla. Magn Reson Med 1996;36:1–6.
24. Zang L-H, Howseman AM, Shulman RG. Assignment of the ^{1}H chemical shift of glycogen. Carbohydrate Res 1991;220:1–9.
25. Zang L-H, Rothman DL, Shulman RG. ^{1}H NMR visibility of mammalian glycogen in solution. Proc Natl Acad Sci USA 1990;87:1678–1680.
26. Behar KL, Rothman DL, Spencer DD, Petroff OAC. Analysis of macromolecule resonances in ^{1}H NMR spectra of human brain. Magn Reson Med 1994;32:294–302.
27. Mason GF, Behar KL, Rothman DL, Shulman RG. NMR determination of intracerebral glucose concentration and transport kinetics in rat brain. J Cereb Blood Flow Metab 1992;12:448–455.
28. Gruetter R, Ugurbil K, Seaquist ER. Steady-state cerebral glucose concentration and transport in the human brain, J Neurochem 1998;70: 397–408.
29. Gruetter R, Rothman DL, Novotny EJ, Shulman GI, Prichard JW, Shulman RG. Detection and assignment of the glucose signal in ^{1}H NMR spectra of the human brain. Magn Reson Med 1992;26:183–188.
30. Nagatomo Y, Wick M, Prielmeier F, Frahm J. Dynamic monitoring of cerebral metabolites during and after transient global ischemia in rats by quantitative proton NMR spectroscopy in vivo. NMR Biomed1995;8: 265–270.
31. Strang RH, Bachelard HS. Extraction, purification and turnover of rat brain glycogen. J Neurochem 1971;18:1067–1076.
32. Chen W, Avison MJ, Bloch G, Shulman RG. Proton NMR observation of glycogen in vivo. Magn Reson Med 1994;31:576–579.
33. Kwee IL, Nakada T, Ellis WG. Elevation in relative levels of brain membrane unsaturated fatty acids in Alzheimer's disease: high resolution proton spectroscopic studies of membrane lipid extracts. Magn Reson Med 1991;21:49–54.
34. Salvan AM, Vion-Dury J, Confort-Gouny S, Dano P, Cozzone PJ. Increased cerebral glycogen detected by localized ^{1}H-magnetic resonance spectroscopy in a patient with suspected McArdle's disease. Eur Neurol 1997;37:251–253.
35. Rothman DL, Hanstock CC, Petroff AC, Novotny EJ, Prichard JW, Shulman RG. Localized ^{1}H NMR spectra of glutamate in the human brain. Magn Reson Med 1992;25:94–106.
36. Ernst T, Hennig J. Coupling effects in volume selectiv ^{1}H spectroscopy of major brain metabolites. Magn Reson Med 1991;21:82–96.
37. Govindaraju V, Basus VJ, Matson GB, Maudsley AA. Measurement of chemical shifts and coupling constants for glutamate and glutamine. Magn Reson Med 1998;39:1011–1013.
38. de Graaf RA, Luo Y, Garwood M, Nicolay K. B_1 -insensitive, single-shot localization and water suppression. J Magn Reson B 1996;113:35–45.
39. Roell SA, Dreher W, Busch E, Leibfritz D. Magnetization transfer attenuates metabolite signals in tumors and contralateral animal brain: In vivo observation by proton NMR spectroscopy. Magn Reson Med 1998;39:742–748.